



A novel series of metabotropic glutamate receptor 5 negative allosteric modulators based on a 4,5,6,7-tetrahydropyrazolo [1,5-*a*]pyridine core



Guillaume Duvey^a, Benjamin Perry^{a,*}, Emmanuel Le Poul^a, Sonia Poli^a, Beatrice Bonnet^a, Nathalie Lambeng^a, Delphine Charvin^a, Tansy Donovan-Rodrigues^a, Hasnaà Haddouk^a, Stefania Gagliardi^b, Jean-Philippe Rocher^a

^aAddex Therapeutics, 12 Chemin des Aulx, Plan-les-Ouates 1228, Geneva, Switzerland

^bNiKem Research s.r.l., Via Zambelletti 25, 20021 Barazante (MI), Italy

ARTICLE INFO

Article history:

Received 30 May 2013

Revised 12 June 2013

Accepted 16 June 2013

Available online 25 June 2013

Keywords:

mGlu5

Metabotropic

Pain

Glutamate

Allosteric

ABSTRACT

A series of potent non-acetylinic negative allosteric modulators of the metabotropic glutamate receptor 5 (mGlu5 NAMs) was developed starting from HTS screening hit **1**. Potency was improved via iterative SAR, and physicochemical properties were optimized to deliver orally bioavailable compounds acceptable for in vivo testing. A lead molecule from the series demonstrated dose-dependent activity in the second phase of the rat formalin test from 30 mg/kg, and a preliminary PK/PD relationship was established.

© 2013 Elsevier Ltd. All rights reserved.

mGlu5 is a family I G_q-coupled metabotropic glutamate receptor expressed both peripherally and within the CNS, primarily postsynaptically in the limbic cortex, hippocampus, amygdala, basal ganglia, thalamus and olfactory tubercle.¹ mGlu5 has been the target of significant drug discovery efforts due to its implications in numerous, varied indications such as migraine, Fragile X syndrome, chronic pain, gastroesophageal reflux disease (GERD) and Parkinson's disease.² The majority of this work has focused on negative allosteric modulators (NAMs) of mGlu5 receptor such as MTEP, mavoglurant and dipraglurant (Fig. 1).^{3–5} With the intention of identifying novel mGlu5 receptor NAM pharmacophores, a high throughput screen of the Addex corporate library was performed (ca. 70,000 molecules) using a FLIPR-based Ca²⁺ release assay.⁶ Amongst the hits identified was 4,5,6,7-tetrahydropyrazolo[1,5-*a*]pyridine **1**, which afforded full inhibitory modulation with an IC₅₀ of 1.3 μM. Subsequent validation of this molecule in an mGlu5 receptor rat cortex binding assay (³H-MPEP) showed a binding IC₅₀ of 1.2 μM. Further profiling showed this hit compound to have a good solubility in kinetic solubility assays (0.17 and 0.18 mg/mL at pH 1.0 and 7.4 respectively), no major issue in CYP inhibition (no inhibitory IC₅₀ >10 μM on 4 major CYP isoforms), however

the compound suffered high intrinsic clearance in both human and rat microsomes (97 and 118 μL/min/mg prot. respectively). As such, it was decided to further investigate this chemotype with view to identifying compounds displaying improved potency and in vitro microsomal stability.

Initial investigation focused on the nature of the link between the pyridine ring and 4,5,6,7-tetrahydropyrazolo[1,5-*a*]pyridine core, in order to find the optimal distance between these two motifs in terms of potency. Various linkers were investigated in this position, the majority of which were inactive. Those that were found active are shown in Table 1; these optimal linkers were of 2-atom lengths bearing either a carbonyl or ether functionality at the linking position with the 4,5,6,7-tetrahydropyrazolo[1,5-*a*]pyridine core (ether **2**, ketone **3** and amide **4**). Reversing the amide or ether resulted in inactive compounds, as did extending or reducing chain length. It is postulated that an element of conjugation between the two aromatic systems due to linker tautomerism may be a significant potency driver; amide **4**, capable of a tautomeric form where the linker is a double bond, is active whereas substituted amide **5** is inactive. Likewise ketone **3**, which is observed as a 2:3 mixture between tautomeric enol ether and ketone in 1D ¹H NMR, is rather potent. It is plausible that these pseudo-conjugated linkers may be occupying the same area of the mGlu5 receptor NAM pharmacophore as the classic acetylene linker

* Corresponding author.

E-mail address: benjamin.perry@addexpharma.com (B. Perry).

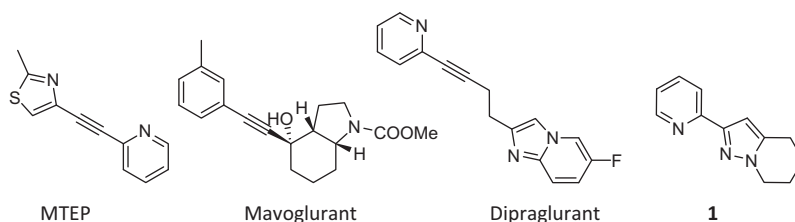


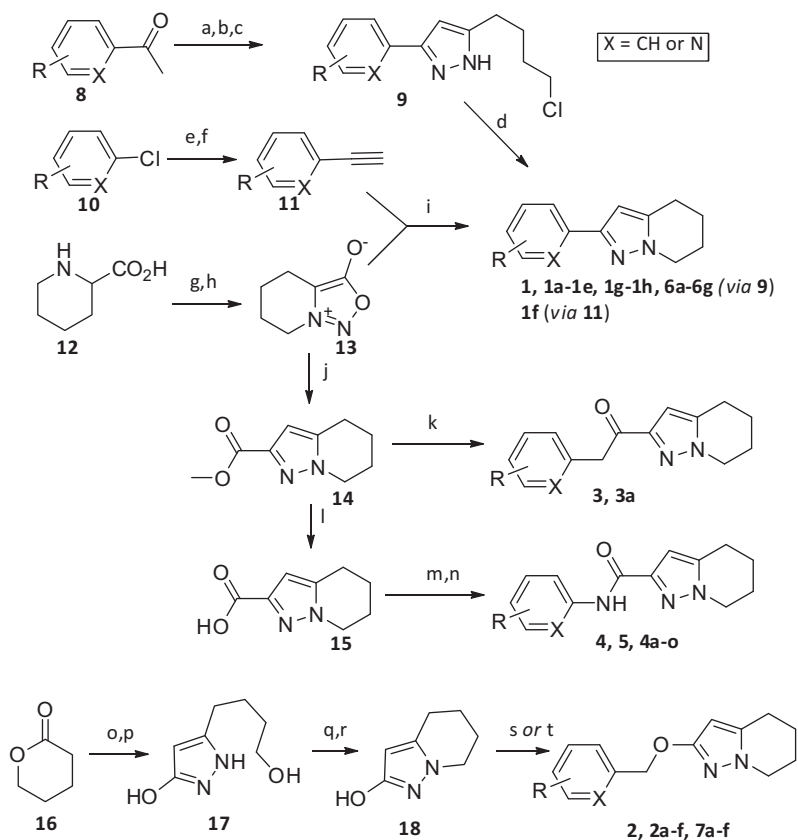
Figure 1. Known mGlu5 NAMs and HTS screening hit **1**.

Table 1
Investigation of the linker space between aromatic rings

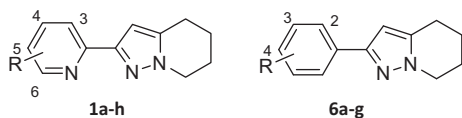
Compound	1	2	3	4	5
Linker	-	$-(CH_2)_n-O-$	$-(CH_2)_n-C(=O)-$	$-NH-C(=O)-$	$-N(CH_3)-C(=O)-$
FLIPR rmGlu5 IC ₅₀ (nM)	1292	2498	390	364	NA

present in many of the known mGlu5 receptor NAMs. It should be noted that only one stereoisomer of the enol was observed by 1D ¹H NMR (*E/Z* stereochemistry not determined).

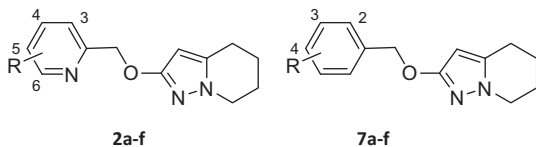
Representative synthesis of the various linked compounds is shown in **Scheme 1**. Direct-linked analogues **1**, **1a–e** and **6a–g** can be synthesized in 4 steps from substituted 2-acetylpyridines or acetylbenzenes via pyrazoles **9** followed by ring closure. In an alternative route to generate **1f**, key intermediate 4,5,6,7-tetrahydro-[1,2,3]oxadiazolo[3,4-*a*]pyridin-8-ium-3-olate (**13**) is generated in two steps from piperidine-2-carboxylic acid **12**.⁷ Reaction of this intermediate with various 2-acetylinyl-pyridines or phenylacetylenes generates the direct-linked compounds via a [3+2]cycloaddition. Reaction of key intermediate **13** with methyl propiolate generates ester **14**, which can either be reacted with methylpyridines under basic conditions to give ketone-linked **3** and **3a**, or saponified and coupled with amines to generate amides **4**, **5** and **4a–o**. Ester-linked compounds are generated using an



Scheme 1. Reagents and conditions: (a) Me₂NNH₂, EtOH, reflux, 37–92%; (b) LDA, THF, –78 °C then 5-chlorovalerylchloride, –78 to 0 °C; (c) hydrazine mono-hydrate, EtOH; reflux 35–66% over 2 steps; (d) NaH, THF, 0 °C, 30–51%; (e) TMSCH, Pd(PPh₃)₂Cl₂, CuI, TEA, DCM, 80 °C, 84%; (f) KOH, MeOH, DCM, rt, 34%; (g) NaNO₂, HCl, 0 °C; (h) TFAA, THF, rt; 63% over 2 steps (i) xylene, reflux, 67%; (j) methyl propiolate, xylene, reflux, 85%; (k) substituted 2-methyl pyridine, KHMDS, THF, –78 °C to rt, 64–88%; (l) KOH, MeOH, RT, 78%; (m) (COCl)₂, DMF, DCM, RT; (n) substituted 2-aminopyridine, pyridine, RT, 60–80% over 2 steps; (o) EtOAc, Na, EtOH, RT; (p) hydrazine mono-hydrate, EtOH, 40 °C, 77% over 2 steps; (q) HBr, H₂SO₄, reflux; (r) NaOH, rt, 57% over 2 steps; (s) substituted 2-halomethylpyridine/benzyl halide, NaH, DMF, 0 °C to rt 5–51%; (t) substituted 2-hydroxymethyl pyridine/benzyl alcohol, PBu₃, THF, (pipCON)₂.

Table 2
Scanning of aryl ring in direct-linked series

Compound	R	FLIPR rmGlu5 IC ₅₀ (nM)
1	H	1292
1a	3-Me	NA
1b	4-Me	3075
1c	4-Cl	675
1d	5-Me	3003
1e	5-Cl	669
1f	5-CN	>10,000
1g	6-Me	1243
1h	6-Cl	1516
6a	H	1895
6b	2-Cl	2648
6c	3-Cl	77
6d	4-Cl	4232
6e	3-CF ₃	3994
6f	3-OMe	4503
6g	3-F	1573

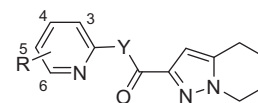
Table 3
Scanning of aryl ring in ether-linked series

Compound	R	FLIPR rmGlu5 IC ₅₀ (nM)
2	H	2498
2a	4-Cl	>10,000
2b	5-CN	316
2c	5-Cl	1548
2d	5-Ac	NA
2e	6-Cl	5897
2f	6-NH ₂	NA
7a	H	NA
7b	2-CN	NA
7c	3-Me	769
7d	3-Cl	332 ^a
7e	3-CN	451 ^a
7f	4-CN	1612

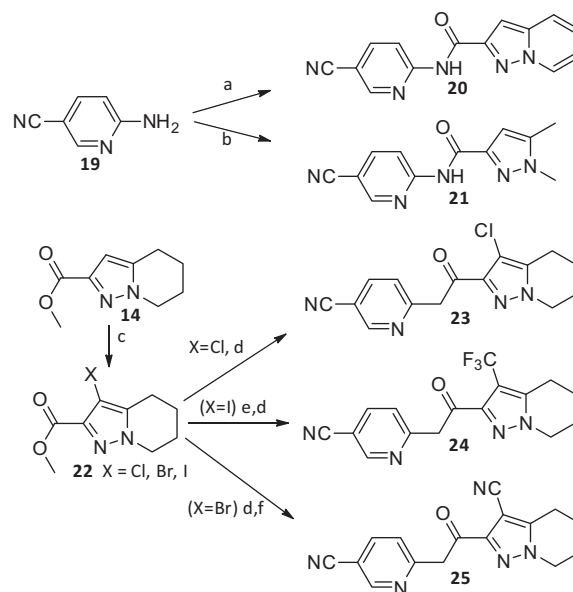
^a Compounds displayed partial negative allosteric modulatory activity, with max % inhibition between 60% and 70%.

alternative pathway. Ring opening of delta lactone **16** with ethyl acetate in the presence of LiHMDS, followed by hydrazine condensation gives 3-hydroxy-(5-butan-4-ol)-pyrazole **17**. This product was cyclized to give 2-hydroxy-4,5,6,7-tetrahydropyrazolo[1,5-a]pyridine **18**. Alkylation of this hydroxyl group led to ether-linked products **2**, **2a–f** and **7a–f**.

Investigation of substitution and modulation of the pyridine ring was undertaken for the direct linker, ether linker, amide linker and ketone linker (Tables 2–4). A variety of substitution of the pyridine ring, along with switching from pyridine to substituted phenyl ring, is tolerated. For the direct-linked and ether linked compounds, the *m*-chloro-phenyl analogue such as in compound **6c** led to greater potency while the 5-cyano pyridinyl left hand side as in **2b** is preferred. This SAR observed in the pyridinyl series can be transferred to the amido linker subseries. Interestingly, certain of the ether linked compounds bearing a 3-substituted phenyl ring displayed only partial modulatory activity (**7d**, **7e**). From

Table 4
Scanning of aryl ring in amide and ketone-linked series

Compound	Y	R	FLIPR rmGlu5 IC ₅₀ (nM)
4	NH	H	364
4a	NH	3-CN	NA
4b	NH	3-Me	NA
4c	NH	3-OMe	NA
4d	NH	3-NH ₂	>10,000
4e	NH	3-OH	>10,000
4f	NH	4-CN	NA
4g	NH	4-Me	NA
4h	NH	5-CN	90
4i	NH	5-F	60
4j	NH	5-NH ₂	NA
4k	NH	5-Cl	262
4l	NH	6-Me	NA
4m	NH	6-OMe	NA
4n	NH	6-CF ₃	NA
4o	NH	6-F	4744
3	CH ₂	H	390
3a	CH ₂	5-CN	53



Scheme 2. Reagents and conditions: (a) pyrazolo[1,5-a]pyridine-2-yl carbonyl chloride, pyridine, rt, 34%; (b) 1,5-dimethyl-1H-pyrazole-3-carbonyl chloride, pyridine, RT, 45%; (c) NXS, MeCN, 80–100 °C, 55–95%; (d) 5-cyano-2-methyl pyridine, KHMDS, THF, –78 °C to rt, 5–14%; (e) MeO₂CCF₂SO₂F, CuI, DMF, 100 °C, 68%; (f) CuI, KI, NaCN, MeNHCH₂CH₂NHMe, PhMe, 150 °C, 17%.

Table 5
Substitution of the 3-position of 4,5,6,7-tetrahydropyrazolo[1,5-a]pyridine

Compound	20	21	23	24	25
FLIPR rmGlu5 IC ₅₀ (nM)	1806	2620	108	7178	5377

comparison of **2a**, **2e** and **7d** it can be seen that SAR was not entirely transferable between phenyl and pyridinyl left-hand side. For the amide-linked compounds, 5-cyano and 5-fluoro substituted pyridines were most favored in terms of potency (**4h**, **4i**), whilst

Table 6
[³H]MPEP binding and ADMET profiling of key compounds

Cpd ID	1	6c	2b	4h	4i	3a	21	23
FLIPR rat mGlu5 IC ₅₀ (nM) ^a	1292	77	316	90	60	53	2620	108
Rat cortex [³ H]MPEP binding (nM)	1180	401	299	151	166	139	n.d.	n.d.
CL _{int} Rat/Human (μL/min/mg.prot)	118/97	384/386	42/85	– ^b /83	– ^b /31	108/46	<5/<5	649/79
Solubility (mg/mL) ^c pH 1/pH 7.4	0.17/0.18	0.11/0.02	0.16/0.10	n.d.	0.10/0.04	0.08/0.03	n.d.	n.d.
CYP inhibition (μM)	>10 all	<0.75 on 1A2	>10 all	>10 all	>10 all	>10 all	n.d.	>10 all
3A4/2C9/2D6/1A2	isoforms		isoforms	isoforms	isoforms	isoforms		isoforms

^a All compounds displayed full (>99%) inhibition of mGlu5 at 30 μM.

^b Compound unstable in rat plasma matrix.

^c Kinetic solubility measurement using DMSO solution.

many of the other changes attempted resulted in complete loss of activity; such moieties and steep SAR and are often observed in mGlu5 receptor NAM chemical series, with fluoro-, chloro- and cyano-substituted pyridines being regularly found amongst the most potent molecules in other mGlu5 receptor NAM series.^{3–5} This further reinforces the likely overlap of pharmacophoric space between this series and those of the acetylene-containing series. Transfer of these active motifs to the ketone linker resulted in the most potent compound in this series, **3a**.

Finally, investigation of the 4,5,6,7-tetrahydropyrazolo[1,5-*a*]pyridine core was conducted (Scheme 2, Table 5). Substitution of the 3-position of the 4,5,6,7-tetrahydropyrazolo[1,5-*a*]pyridine for ketone linked compounds showed that whilst substitution of this position was tolerated, a general trend towards decreased activity was observed for such compounds (**23–25**). It is also shown that aromatization or ring opening of the 6 membered saturated ring of the 4,5,6,7-tetrahydropyrazolo[1,5-*a*]pyridine is detrimental to potency (**20, 21**).

Rat cortex binding studies were performed on key compounds using known mGlu5 allosteric ligand [³H]MPEP.⁶ Similar levels of potency, were seen between functional activity in the FLIPR Ca²⁺ release assay (Table 6), suggesting that this series of compound occupies or perturbs the classical allosteric MPEP site on mGlu5.

Profiling of key compounds from this SAR investigation in preliminary in vitro ADME screens showed that the amide, keto and direct branched linker compounds suffered significant metabolic instability in rat microsomes (Table 6). Furthermore, certain amide-linked compounds were shown to be unstable in the assay medium, suggesting rapid hydrolysis of the amide bond. Stability of the compounds profiled in human microsomes suggests discrepancy between the two species, with most compounds, amide-linked included, being significantly more stable in human. The much improved stability of **21** demonstrates that the saturated ring of the core heterocycle is likely a major site of metabolism. Only compound **2b** of the ether linked compounds displayed a sufficiently acceptable in vitro intrinsic microsomal clearance in rat to progress to PK studies. All compounds displayed good solubilities and with the exception of direct-linked compound **6c** there were no recurring major flags in CYP inhibition on 4 major isoforms.

3 mg/kg iv administration of compound **2b** to rat showed this compound to have a high clearance and moderate volume of

Table 7
Pharmacokinetics of **2b** in rats

Rat PK 3 mg/kg iv ^a	CL (mL/min/kg)	72
	V _{ss} (L/kg)	1.1
	T _{1/2} (h)	0.2
Rat PK 30 mg/kg sc ^b	C _{Max} (ng/mL) Plasma	2896
	C _{Max} (ng/mL) CSF	416
	C _{Max} CSF/Plasma (%)	14.4

^a Results are mean of 3 animals.

^b Results are mean of 4 animals.

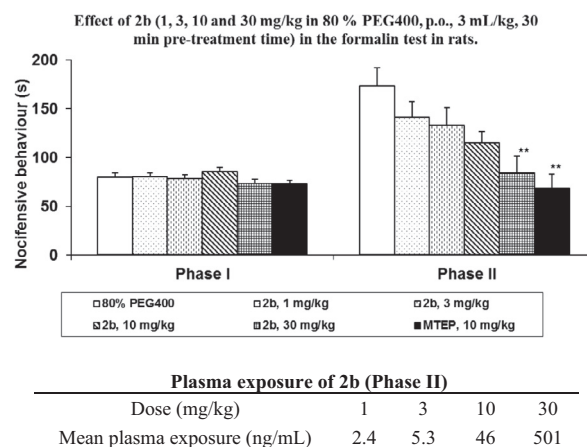


Figure 2. Effect of **2b** (1, 3, 10 and 30 mg/kg in 80% PEG400, p.o., 3 mL/kg, 30 min pre-treatment time) in the formalin test in Sprague–Dawley rats (*n* = 10/group). Each point represents the observed mean (+SEM). ***p* < 0.01 compared with 80% PEG400 in Phase II.

distribution resulting in a short half-life (Table 7). 30 mg/kg sc with continuous CSF sampling suggested a one compartmental behaviour between plasma and CSF, with a moderate-high CSF/plasma ratio similar to the in vitro measured plasma free fraction (rat PPB *f*_u = 32%). Therefore, it was decided to profile compound **2b** in the biphasic rat formalin model of nociception.⁸ mGlu5 receptor is implicated in the processing of nociceptive behavior,⁹ and mGlu5 receptor NAM MTEP has been shown to be active in reducing nociceptive behavior induced by formalin.¹⁰ Indeed, orally dosed compound **2b** (1, 3, 10, 30 mg/kg) showed dose dependent reduction of nociceptive behaviour in Phase II (1 h post injection) but not Phase I of the formalin test (Fig. 2), with significant effect being observed at 30 mg/kg dose, the maximum effect being of equal magnitude to that seen with positive control MTEP. Terminal plasma concentrations of compound **2b** showed dose-proportional exposure of the compound, with only the 30 mg/kg dose demonstrating an exposure of sufficient magnitude for compound **2b** to be exposed at levels close to the IC₅₀ value in the brain.¹¹ This confirms that compound **2b** is orally bioavailable and strongly suggests the compound is capable of blocking mGlu5 receptor in vivo. It is postulated that the anti-nociceptive trend observed at each dose may be due to exposure of the compound during the early stages of the experiment, and that mGlu5 blockade has a delayed-response anti-nociceptive effect in the formalin test in rat.

In conclusion, we have identified a novel mGlu5 receptor NAM chemotype with postulated overlap with the MPEP/MTEP pharmacophoric space. Optimization of each area of the hit molecule resulted in identification of several sub-100 nM compounds. Molecules from this series are highly soluble and brain penetrant,

and the potential for in vivo efficacy from this series has been demonstrated by lead molecule **2b** in the rat formalin test. Further investigation and optimization of this series is ongoing focused on improving in vivo PK profile (improving clearance via reduction of plasma free fraction, improving exposure) and improving potency.

Acknowledgments

We would like to acknowledge the indispensable technical contributions of V. Nhem, R. Furnari, H. Faure, A. Bessif, S. Charreton, B. Mingard, A. Riu, P. Bazzy, and C. Pesenti, and thank M. Kalinichev and I. Urios for data analysis.

Supplementary data

Supplementary data associated with this article can be found, in the online version, at <http://dx.doi.org/10.1016/j.bmcl.2013.06.044>.

References and notes

1. Spooren, W.; Ballard, T.; Gasparini, F.; Amalric, M.; Mutel, V.; Schreiber, R. *Behav. Pharmacol.* **2003**, *14*, 257.
2. Jaeschke, G.; Wettstein, J. G.; Nordquist, R. E.; Spooren, W. *Expert Opin. Ther. Pat.* **2008**, *18*, 123.
3. Rocher, J. P.; Bonnet, B.; Bolea, C.; Lutjens, R.; Le Poul, E.; Poli, S.; Epping-Jordan, M.; Bessis, A. S.; Ludwig, B.; Mutel, V. *Curr. Top. Med. Chem.* **2011**, *11*, 680.
4. Emmitte, K. A. *ACS Chem. Neurosci.* **2011**, *2*, 411.
5. Célanire, S.; Duvey, G.; Poli, S.; Rocher, J. P. *Annual Reports in Medicinal Chemistry In Desai, M. C., Ed.; Academic Press Elsevier, 2012; 47, p 71.*
6. See Supplementary data for assay conditions.
7. Venkatesan, A. M.; Agarwal, A.; Abe, T.; Ushiroguchi, H.; Yamamura, I.; Ado, M.; Tsuyoshi, T.; Dos, S. O.; Gu, Y.; Sum, F. W.; Li, Z.; Francisco, G.; Lin, Y. I.; Petersen, P. J.; Yang, Y.; Kumagai, T.; Weiss, W. J.; Shlaes, D. M.; Knox, J. R.; Mansour, T. S. *J. Med. Chem.* **2006**, *49*, 4623.
8. Tjølsen, A.; Berge, O. G.; Hunskaar, S.; Rosland, J. H.; Hole, K. *Pain* **1992**, *51*, 5.
9. Kolber, B. J.; Montana, M. C.; Carrasquillo, Y.; Xu, J.; Heinemann, S. F.; Muglia, L. J.; Gereau, R. W. *J. Neurosci.* **2010**, *30*, 8203.
10. Sevostianova, N.; Danysz, W. *Neuropharmacology* **2006**, *51*, 623.
11. Extrapolation of brain concentration of **2b** based on observed plasma exposure during experiment and CSF/plasma ratio from sc PK experiment suggest brain concentration for 30 mg/kg dose would be 95 ng/mL = 375 nM.